SIMULATION OF SEMICONDUCTOR DEVICES AND PROCESSES Vol. 3
Edited by G. Baccarani, M. Rudan - Bologna (Italy) September 26-28, 1988 - Tecnoprint

NEAR BALLISTIC TRANSPORTS IN SWITCHING OPERATIONS OF GaAs MESFET'S WITH A SUBMICROMETER GATE-LENGTH OBSERVED BY MULTI-PARTICLE SIMULATION

Y. Yamada, N. Shimojoh

Department of Electrical Engineering and Computer Sciences
Kumamoto University, Kumamoto 860, Japan

SUMMARY

Here we study near ballistic transports proper to switching operations of GaAs MESFET's with a 0.5 μm gate-length, using a multi-particle simulator. The time-resolved distributions of electron velocity, electron energy, electric-field and carrier density along the channel related with ON↔OFF operations are obtained, in addition to time responses of the currents. The near ballistic transports proper to the ON↔OFF operations are significant near the source electrode and underneath the gate. The dynamics of the particles in upper valleys which determines the switching time is depicted. It is tried to evaluate the relaxation times of momentum and energy both from their time responses and from the steady state distributions of velocity, energy and so on. It is found that the well-known ballance equations of momentum and energy underestimates electron energy and overestimates electron velocity underneath the gate.

INTRODUCTION

Recently a multi-particle simulator, which can exactly take into account near ballistic transports in submicrometer gate GaAs MESFETs, has been widely applied to evaluation of the characteristics. However few reports have been published on details of electron dynamics in switching operations, although there is only a few papers on calculation of a time response of the drain current and a switching time, which were reported by Yoshii, Tomizawa, and Yokoyama(1983), and Yokoyama, Tomizawa, and Yoshii(1985). It is necessary to publish the details of electron dynamics for modelling and further development of a more tractable method such as relaxation time approximation, which are proposed or simplified by Blotekjaer(1970), Cook and Frey(1982), and Stenzel, Elschner, and Spallek(1987). The relaxation time approximation will be applied to CAD of the

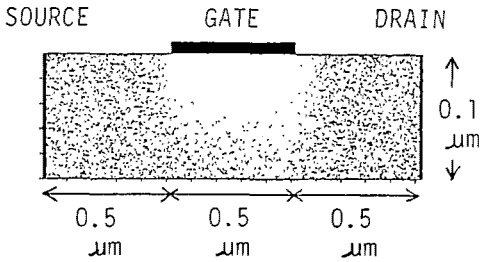

Fig. 1. Schematic drawing of a MESFET device used in the simulation. The small dots denote particles.

device in the near future, because it does not require big computer resources and is able to carry out time-resolved calculation without any numerical noise, in contrast to the multi-particle simulator.

In the present paper, in addition to the time responses of the currents, electron dynamics in the switching operations, such as velocity, energy, electric-field, and carrier density, will be depicted in detail. Next the same technique will be applied to observation of relaxation processes of energy and momentum at some points in the device. Finally accuracy of the relaxation time approximation will be discussed through the relaxation times.

MULTI-PARTICLE SIMULATOR

The multi-particle simulator has been applied to the device shown in fig. 1. The doping density of donor is 10^{17} cm^{-3} and lattice temperature is 300 K. The electric-field in the device is self-consistently calculated with the particle distribution through Poisson's equation. The Monte Carlo technique used in the present simulation is followed by Fawcett, Boardman, and Swain(1970). Their model for the conduction band is a two-valley one. The number of particles in the device is 10,000 at the initial step of the simulation. Figure 1 shows a steady state distribution of particles in a ON state which are denoted by small dots.

NEAR BALLISTIC TRANSPORTS IN SWITCHING OPERATIONS

Figure 2 shows a scheme of the switching operation of the gate voltage(V_G) and the corresponding time-responses of the source current(I_S) and the drain current(I_D). The drain voltage (V_D) is 1.0 V. The currents consist of drift and displacement currents. The drift component is dominant at the source and drain, while the displacement component is dominant at the gate. The multi-particle simulator causes large numerical noise in the calculated results, especially in the transient data. In addition, the currents at the source, gate, and drain electrodes are not instantaneously ballanced due to the numerical noise. However we can find out features of the transports during the

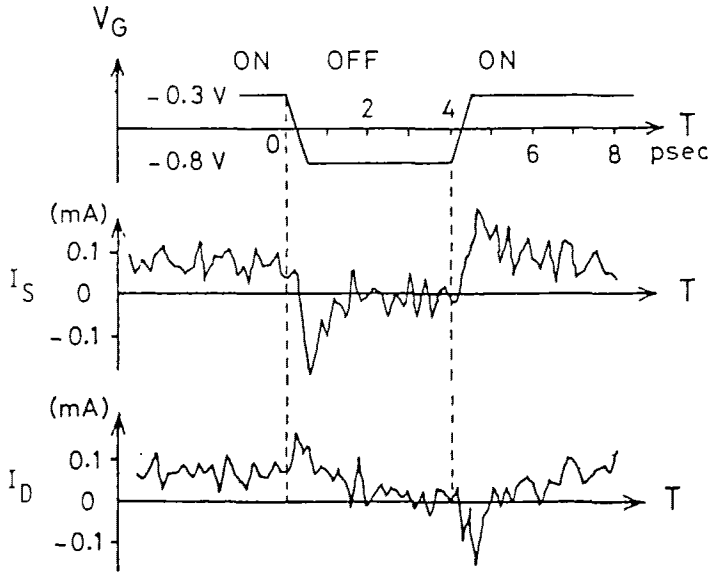

Fig. 2. A scheme of switching operation and the time responses of the source current(I_S) and drain current(I_D).

switching operations. The switching time in fig. 2 is 3-4 psec. The figures from fig. 3 to fig. 8 show the time-resolved distributions of velocity, energy, electric-field, and carrier density just after the switching near the bottom of the channel. Here the velocity and electric-field are parallel to the channel.

First let us observe the transports during the ON → OFF operation. For time less than 1 psec, the particles in a lower valley in the source side underneath the gate ballistically move toward the source due to the negative field more than -10 kV/cm, but they do not change into upper valleys, as shown in figs. 3 (b) and 3(e), due to the rather small amplitude of V_G. Their velocity exceeds 4×10^7 cm/s instantaneously, which is close to the maximum velocity of the ON steady state. In the drain side there are many particles in the upper valleys in the ON steady state. They do not almost change their behaviours during the small period in spite of large change of the electric-field there, because their effective mass is very large. It takes more than 3 psec for them to be cooled in to a lower valley. The undershoot and overshoot in the time responses of I_S and I_D, respectively, and the slow variation of I_D just after the overshoot reflect the above transports.

Next let us see the transports during the OFF → ON operation. We observe two kinds of near ballistic transports near the source electrode and underneath the gate. The one occures at about 4.44 psec near the source electrode due to the electric-field of about 6 kV/cm shown in fig. 5. This transport is shown in the enlarged figure of fig. 6. The accelerated particles are

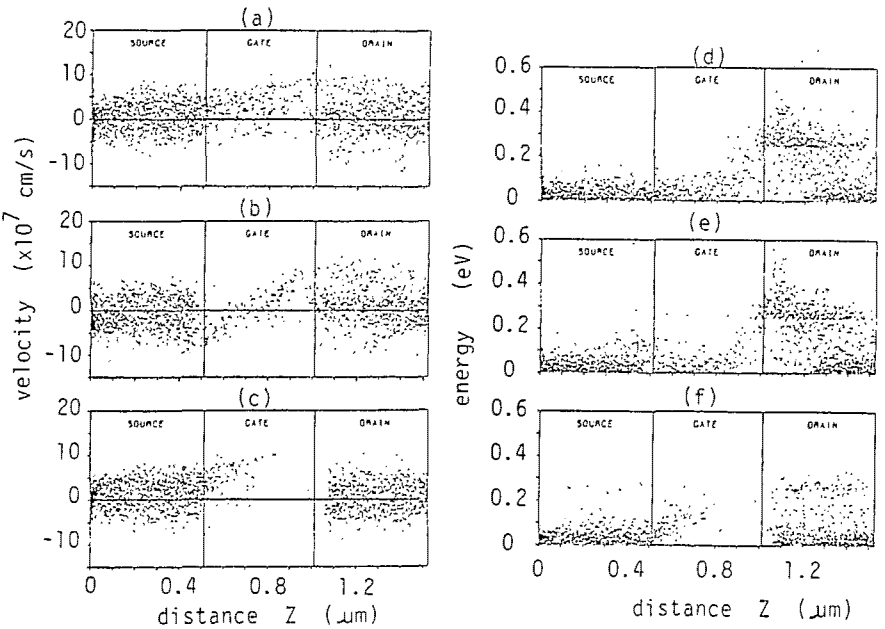

Fig. 3. The distributions of particle velocity parallel to the channel and particle energy in the ON steady state((a), (d)), at 0.73 psec((b),(e)), and at 4.70 psec((c),(f)).

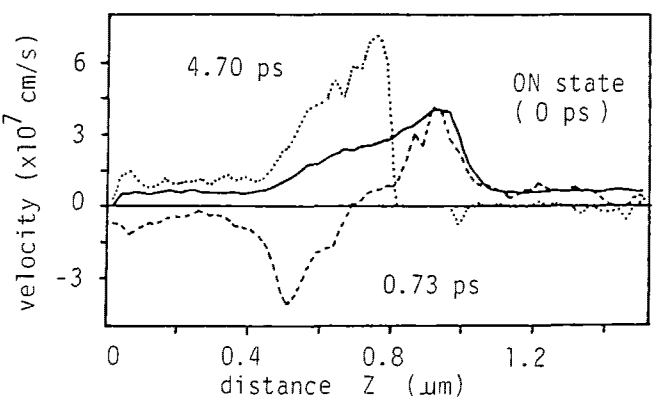

Fig. 4. The distributions of average velocity parallel to the channel along the bottom of the channel in the ON steady state, at 0.73 psec, and at 4.70 psec.

not perfectly cooled at the source side under the gate. The another near ballistic transport starts after about 4.4 psec under the gate. The particles in the lower valley which reach the source side under the gate are again accelerated by the electric-field of about 12 kV/cm shown in fig. 5 and move toward the drain ballistically. Their velocity reaches about 7×10^{17} cm/s as shown in fig. 4, which is fairly larger than the

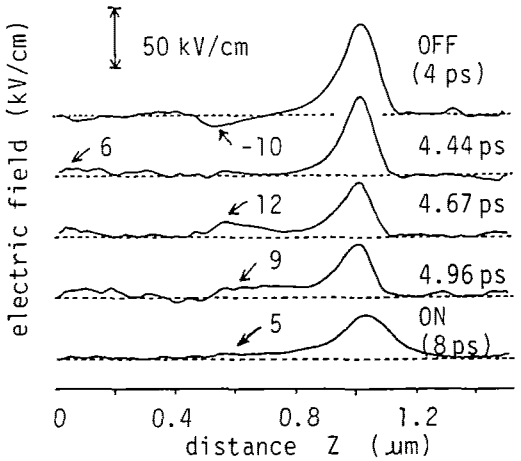

Fig. 5. The time-resolved distributions of electric-field parallel to the channel along the bottom of the channel in the OFF state(4 psec), at 4.44 psec, at 4.67 psec, at 4.96 psec, and in the ON state(8 psec).

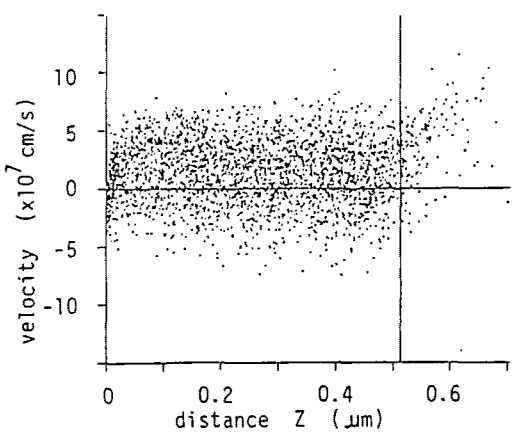

Fig. 6. The distribution of particle velocity parallel to the channel near the source electrode. The velocities of particles sharply rise in the neighbourhood of the source electrode and relax hereafter.

maximum velocity of the ON state. This accelerating electric-field decreases as the number of particles coming into the region under the gate increases. After about 5.5 psec the fastest particles reach the drain edge of the channel under the gate. Most of these particles are scattered into upper valleys due to inter-valley scatterings. First the generation of the particles in the upper valleys occures at the bottom of the

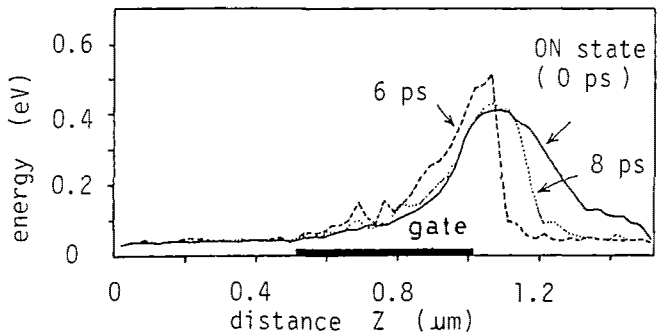

Fig. 7. The time-resolved distributions of average energy along the bottom of the channel at 6 psec, at 8 psec, and in the ON steady state during the OFF → ON operation.

channel and then the particles slowly drift toward the drain and upward due to their large effective mass. Finally they are cooled into the lower valley as they come close to the drain electrode. It takes more than 4 psec for their distribution of energy to reach the steady state one, as shown in fig. 7. Thus, the transports described above are cleary reflected in the overshoot and undershoot of I_S and I_D, respectively, and the slow variation of I_D just after the undershoot.

Thus, the slow responses of I_D just after the overshoot and undershoot are responsible for the slow movements of the particles in the upper valleys. Perhaps the responses may depend on V_D, because the population of the upper valleys

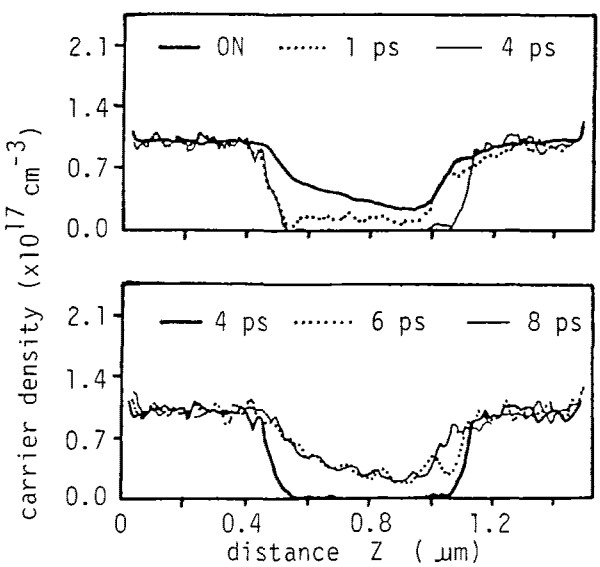

Fig. 8. The time-resolved distributions of carrier density along the bottom of the channel in a sequence of the ON → OFF → ON operation.

increases with V_D.

Figure 8 shows the time-resolved distributions of carrier density along the bottom of the channel. In the ON → OFF switching, the particles in the middle of the channel under the gate do not quickly move due to the almost zero electric-field there. In the OFF → ON switching, the particles temporary accumulate at the drain edge of the channel under the gate due to intervalley scattering, as shown by the dotted line, because there are no particles under the gate in the OFF state, and the accumulation vanishes as the many particles in the upper valleys drift toward the drain.

RELAXATION OF ENERGY AND MOMENTUM IN THE DEVICE

Next we have simulated the relaxation of energy and momentum in the device. In this simulation, the drain voltage is changed suddenly from 1.0 V(ON state) to zero. The gate voltage remains constant(-0.3 V) during the simulation.

Figures 9(a)-9(d) show the time-resolved distributions of the carrier density, electric field, momentum and energy along the bottom of the channel. The electric-field and momentum are parallel to the channel. The carrier density, electric-field, and momentum quickly relax within 0.7 psec, while the energy slowly relaxes.

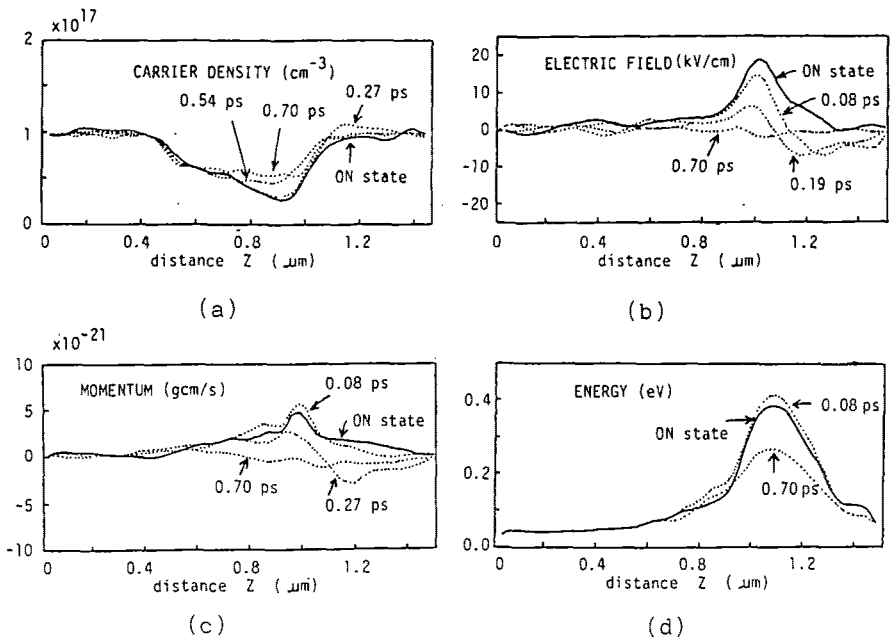

Fig. 9. The time-resolved distributions of carrier density(a), electric-field(b) and momentum(c) parallel to the channel, and energy(d) in the relaxation.

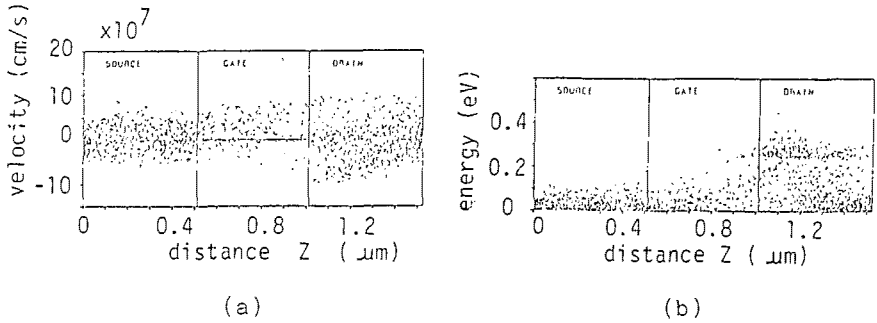

(a) (b)

Fig. 10. The distributions of particle velocity(a) and energy (b) at 0.22 psec after the switching. The velocity is parallel to the channel.

Figures 10(a) and 10(b) show the distributions of velocity and energy of all the particles in the device, respectively, at 0.22 psec after the switching. The velocity is parallel to the channel. The particles in the lower valley near the drain drift backward by the negative field ballistically. The instantaneous increase of the energy shown in fig. 9(d) is caused by this particle behaviour. On the other hand the particles in the upper valleys hardly change their behaviour in this period.

Figure 11(a) shows the time responses of momentum at three points in the device which are denoted by the solid lines. Their energies just before the switching are listed in the figure. Although the carrier density and the energy vary somewhat in this period, we have estimated the time constants for fig. 11(a) taking into account variation of the electric-field only. The time constants are shown by the closed circles in fig.12. They are smaller than the relaxation time of momentum(τ_p) obtained from steady state data by an ensemble Monte carlo simulation for an uniform electric-field case. The τ_p is shown by the dotted line in fig. 12. Figure 11(b) shows the time responses of energy and population of the lower valley. The time responses at two points with the almost same energy in the ON state are shown together in the figure. As it is considered that the variations of the carrier density and the electric-field almost vanish within about 0.70 psec after the switching, we have simply considered that the time constants in fig. 11(b) correspond to the relaxation time of energy. The open circles in fig. 12 show the time constants. They qualitatively agree with the solid line which are the relaxation time of energy(τ_ε) obtained from the same method as the dotted line.

We have shown the time-resolved distributions of the carrier density, the electric-field, the momentum and the energy in the relaxation. The present results may be useful for discussion about accuracy of the relaxation time approximation cited in INTRODUCTION.

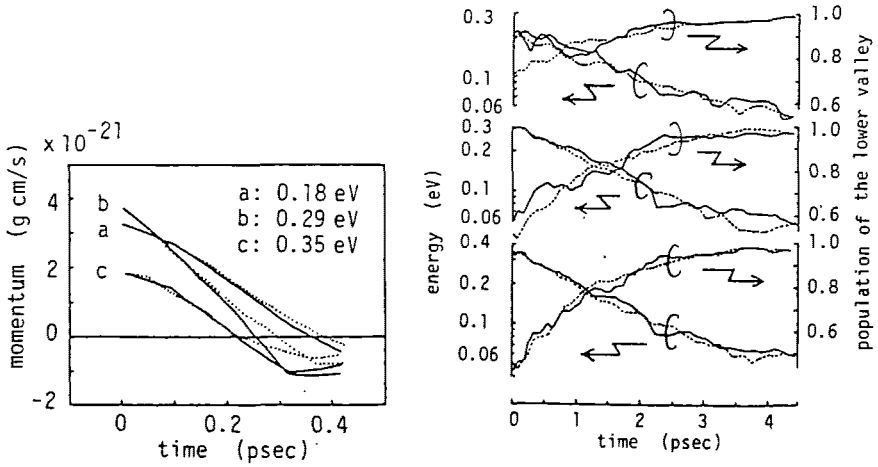

(a) (b)

Fig. 11. (a) The time responses of momentum parallel to the channel for a step-like switching of $V_D \rightarrow 0$ at some points in the device. The dotted lines denote theoretical results calculated with the time constants shown in fig. 12. (b) The time responses of energy and population of the lower vally for the same switching as (a). The responses for the two points with the almost same energy just before the switching are shown together in each figures by the solid and dotted lines.

TRANSPORT EQUATIONS WITH RELAXATION TIMES OF ENERGY AND MOMENTUM

It is not easy, however, to study on accuracy of the relaxation time approximation directly from the transient simulation. In the present work we will simply discuss it from the steady state data of the present work.

It is well known that Blotekjaer(1970) derived transport equations for description of near ballistic transports in GaAs, and Cook and Frey(1982) developed a tractable set of the equations. Their equations are written in steady state as follows.

$$w = \tau_p \left[e\mathbb{F} - \nabla(2\mathcal{E}/3) - (2\mathcal{E}/3n)\nabla n \right] / m^* \quad (1)$$

$$w \cdot \nabla(5\mathcal{E}/3) = e w \cdot \mathbb{F} - (\mathcal{E} - \mathcal{E}_0)/\tau_\mathcal{E} \quad (2)$$

Here the notations have usual meanings. The equations were derived with the assumptions of the displaced Maxwellian distributions and of neglecting the kinetic energy of electron drift compared with the thermal kinetic energy. Naturally the latter assumption is valid near the source and drain sides away from the gate. The contribution of the kinetic energy of electron drift to the total energy, however, reaches about 20 % under the gate in the ON state described in the former sections due to the near ballistic transports.

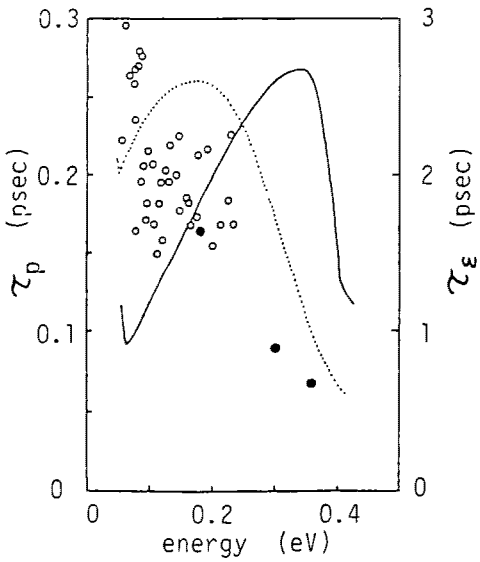

Fig. 12. The relaxation times of energy and momentum and the time constants evaluated from the time responses of energy and momentum. The solid and dotted lines denote τ_ε and τ_p obtained from steady state data in an ensemble Monte Carlo simulation for an uniform electric field case. The open and closed circles show the time constants of energy and momentum evaluated from their time responses by the simulation, respectively.

Using the equations and noticing the boundary conditions for particle dynamics, let us evaluate τ_ε and τ_p from the ON steady state through Eqs. (1) and (2).

First we have evaluated τ_ε and τ_p from the data on the drain side of the peak of energy. Although the values of τ_ε are fairly scattered , they are in good agreement with the solid line in fig. 12 in the range of $0 < \varepsilon < 0.4$ eV. On the other hand, the values of τ_p are considerably small in comparison with the dotted line. It is considered that the small values is due to the thermal equilibrium condition in the drain electrode. Thus, the influence of the drain electrode on τ_ε is small, but it on τ_p extends inside.

The situation changes drastically in the source side of the peak of energy, namely under the gate. Figure 13 shows the values of α_ε and α_p which are defined by $\alpha_\varepsilon = 1-(5/3)\, w \cdot \nabla\varepsilon / w \cdot F$ and $\alpha_p = 1-(2/3)[\, \partial\varepsilon/\partial z + (\varepsilon/n)\, \partial n/\partial z \,]/qF_z$, respectively. Then τ_ε and τ_p are written by $(\varepsilon - \varepsilon_0)/(qw \cdot F\, \alpha_\varepsilon)$ and $m^* v_z/(qF_z\, \alpha_p)$. It is obvious that their negative values in fig. 13 are physically meaningless. This means that Eqs. (1) and (2) may underestimate ε and overestimate w under the gate compared with the multi-particle simulation. As the results, Eqs. (1) and (2) may overestimate the drain current. It is considered that the negative values of α_ε and α_p are caused by the assumptions

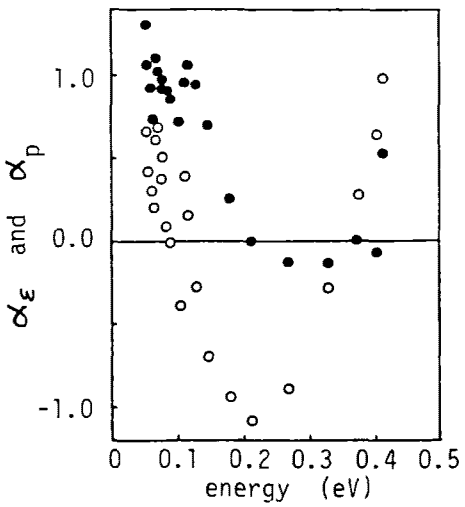

Fig. 13. The energy dependences of α_ε(○) and α_p(●).

in the equations. Thus, the equations are not valid or less accurate under the gate where the near ballistic transport is significant.

A way to simply improve numerical results on the distribution of energy is to use a modified value of τ_ε larger than the original one. The use may make up for the invalid assumptions in Eqs. (1) and (2). The influence of the thermal equilibrium in the drain electrode on the momentum indicates that careless movement of the drain electrode toward the gate, which may be useful for reduction of the number of the particles employed in the simulation, make the average velocity of particles small in the drain side.

DISCUSSION AND CONCLUSIONS

We have presented the time-resolved distributions of energy, velocity, electric-field and carrier density during the ON → OFF switchings, using the multi-particle simulator which self-consistently simulates the particle dynamics and the electric-field. In particular we have depicted the near ballistic transports proper to the ON → OFF switchings. In the initial period of the switchings less than 1 psec, the near ballistic transports of the particles in the lower valley are temporary caused by the large local field. The velocities exceed the maximum velocity in the DC operation. In the OFF → ON switching there are two kinds of the near ballistic transports at the source and under the gate. The slow responses after the period are caused by the particles in the upper valleys. Consequently, the over-all switching-time is strongly dependent on how many particles there are in the upper valleys.

We have also presented the time-resolved data on the relaxation process. The carrier density and momentum quickly

relax within about 0.7 psec, while the energy relaxes very slowly. In the initial period of the relaxation the particles in the lower valley near the drain move ballistically.

Thus, we have shown that the multi-particle simulator is a useful tool for investigation of features of electron dynamics and device performance in the switching operation. It has been found from evaluation of the relaxation times that Eqs. (1) and (2) are less accurate for description of the near ballistic transport under the gate. They underestimate the energy and overestimate the velocity. The drain current may be overestimated by them.

REFERENCES

Blotekjaer K.(1970). Transport Equations for Electrons in Two-Valley Semiconductors. IEEE Trans. Electron Devices, ED-7, pp. 38-47.

Cook R. K. and J. Frey(1982). Two-Dimensional Numerical Simulation of Energy Transport Effects in Si and GaAs MESFET's. IEEE Trans. Electron Devices, ED-29, pp.970-977.

Fawcett W., A. D. Boardman and S. Swain(1970). Monte Carlo Determination of Electron Transport properties in Gallium Arsenide. J. Phys. Chem. Solids, 31, pp. 1963-1990.

Yokoyama K., M. Tomizawa and A. Yoshii(1985). Scaled Performance for Submicron GaAs MESFETs. IEEE Trans. Electron Device Letters, EDL-6, pp. 536-538.

Yoshii A, M. Tomizawa and K. Yokoyama(1983). Accurate Modelling for Submicrometer-gate GaAs MESFET's Using Two-dimensional Particle Simulation. IEEE Trans. Electron Devices, ED-30, pp. 1376-1380.

Stenzel R., H. Elschner and R. Spallek(1987). Numerical Simulation of GaAs MESFETs Including Velocity Overshoot. Solid-State Electronics, 30, pp.873-877.